Supporting Information

Remnant Polarization in Thin Films from a Columnar Liquid Crystal

Carel F.C. Fitié[†], W.S. Christian Roelofs[‡], Martijn Kemerink[,‡] and Rint P. Sijbesma[*,†]*

† Laboratory of Macromolecular and Organic Chemistry, Eindhoven University of Technology, P.O. Box 513, 5600 MB Eindhoven, The Netherlands, and ‡ Applied Physics, Eindhoven University of Technology, P.O. Box 513, 5600 MB, Eindhoven, The Netherlands.

1 Experimental section.

1.1 Materials. All solvents used were of AR quality or better and purchased from Biosolve, Sigma-Aldrich or Acros. All other chemicals were purchased from Sigma-Aldrich. Triethylamine was stored on KOH pellets and $CHCl_3$ was dried over molsieves (4 Å). All other chemicals were used as received.

1.2 Measurements.

*Characterization of **1**.*

^1H NMR and ^{13}C NMR spectra were recorded at room temperature on a Varian Mercury NMR spectrometer (400 MHz for ^1H NMR, 100 MHz for ^{13}C NMR). Proton chemical shifts are reported in ppm downfield from tetramethylsilane ($Si(CH_3)_4$, TMS). Carbon chemical shifts are reported downfield from TMS using the resonance of deuterated chloroform ($CDCl_3$) as internal standard. Matrix-assisted laser desorption ionization time-of-flight mass spectrometry (MALDI-TOF MS) was performed with a PerSeptive Biosystems Voyager-DE PRO spectrometer using an α-cyano-4-hydroxycinnamic acid matrix. Elemental analysis was conducted on a Perkin Elmer 2400.

Phase behaviour and LC structure.

Differential scanning calorimetry (DSC) measurements were performed in hermetic T-zero aluminum sample pans using a TA Instruments Q2000 – 1037 DSC equipped with a RCS90 cooling accessory. The DSC experiments were conducted at a rate of 10 °C/min. All transition temperatures and enthalpies were determined from the first cooling and second heating run using Universal Analysis 2000 software (TA Instruments, USA). The Wide Angle X-ray Scattering (WAXS) patterns for all compounds were measured on a Bruker AXS D8 Discover X-ray diffractometer with a Hi-Star 2D detector using CuKα-radiation (λ = 1.54 Å) filtered by cross-coupled Göbbel mirrors at 40 kV and 40 mA. The sample–detector distance was set at 6 cm. The sample holder was a home-built graphite oven. The temperature was controlled by a thermo-couple and a fast-response power supply (maximum heating rate 300 °C/min), which allowed a temperature range of 25–350 °C. Samples were prepared in a capillary-type glass cell with a diameter of 0.7 mm and a wall thickness of 0.01 mm (Mark-Röhrchen, Germany). The WAXS intensities were corrected by subtracting a background measured with an empty capillary cell.

The Fit2D computer program (version 12.077) was used to integrate the two-dimensional scattering data.[1]

Electro-optical experiments.

For the electro-optical experiments, the BTAs were introduced in LC cells (Linkam, United Kingdom) coated with indium tin oxide (electrode area 0.81 cm^2, cell spacing 5 μm) at 230 °C under a reduced pressure of 20 mbar. Electrical contacts were attached to the sample cells using a highly conductive two-component silver loaded epoxy adhesive (RS Components, United Kingdom) with a maximum operating temperature of 150 °C. During the switching experiments the samples were clamped in a Linkam THMS 600 heating stage and monitored by polarizing optical microscopy (POM) using a Jeneval microscope equipped with crossed polarizers and a Polaroid DMC Ie CCD camera. The input signal (triangular or rectangular wave) was generated with an Agilent 33250A waveform generator and amplified with a Krohn-Hite Corporation model 7600 wideband amplifier. The cell response was measured over a 10 kΩ or 3 kΩ resistor in series with the measurement cell and recorded simultaneously with the input signal using a Tektronix TDS5052B digital oscilloscope. Prior to measurement, all samples were aligned perpendicular (checked by POM) by applying a DC voltage (100-170 V) over the cells at a temperature of 100-150 °C. For the triangular wave measurements, the frequency of the input signal was adjusted so that the cell response just saturated. To determine the spontaneous polarization and coercive field of the samples, the switching peak in the cell response curves was integrated after subtracting a straight baseline between the saturation point and the onset of the peak. Both parameters were determined from the axis crossings of the *P*-*E* loop constructed from the integrated cell response.

For the calculation of the effective dipole moment of per BTA we assumed that all BTA columns are aligned and poled uniformly at the highest field in the triangular wave experiments and that the observed polarization corresponds to a complete reversal of the orientation of the macrodipoles. Under these assumptions, we can simplify the general equation defining the spontaneous polarization in the following manner[2]

$$P_s = \frac{1}{V}\sum_i^N \mu_i = \frac{1}{V_m}\mu \qquad (1)$$

where V_m is the molecular volume of the BTA in the hexagonal columnar phase and μ is the total effective dipole moment of the three amide bonds in each BTA. If we enter the known molecular volume of the BTAs at 150 °C from our WAXS results and the average polarization values in Equation (1), we arrive at a dipole moment of 8.3 ± 2.5 D for **1**.

The polarization lifetime experiments were conducted by first poling the samples uniformly using a 1 s pulse of 200 V after which the field was removed for a period of time t_r. Subsequently, a probe pulse (1 s, 200 V) was applied and the cell response was recorded. The total polarization (P_r) was determined by integrating the current peak from $t = 0$ (application of the probe pulse) up to $t = t_e$ (polarization of the sample completely built-up) after correcting for the RC-contribution (5-10 μs) and the background caused by ohmic conduction. The time t_e was determined as the crossing point of two lines constructed by linear extrapolation of the right edge of the peak and the background signal due to conduction on a double-logarithmic scale (see section 5 for typical response and illustration of the pulse sequence). The saturation value of the polarization (t_r = 100 s) for each cell at 140°C was used to normalize the polarization values obtained for each cell. To determine the characteristic relaxation time for the depolarization process, the data was fitted to a stretched exponential function

$$1 - \frac{P_r}{P_s} = \exp\left[-\left(\frac{t_r}{\tau}\right)^{\beta}\right] \qquad (2)$$

where τ is the characteristic relaxation time of the process and β is a constant ($\beta < 1$). Such functions are commonly used to describe the time dependence of processes that are characterized by a distribution in relaxation times, such as glass transitions.[3-5] As can be seen in Figure 1a in the main text, Equation (2) describes the depolarization process in **1** very well with β-values between 0.4 and 0.6. All data analysis (curve fitting, integration) was performed using OriginPro 8 (OriginLab Corporation, USA).

AFM and SKPM measurements.

Thin films were prepared by spincoating **1** on ITO coated glass substrates (3x3 cm, Naranjo Substrates, Spain) from a chloroform solution (40 mg/ml) at 750 RPM for 60 s. The samples were poled and aligned at 140°C by applying a 10 V potential over the layers for 15 minutes using a drop of mercury as counter electrode. The voltage was removed after the samples had cooled down to 30°C. AFM and SKPM measurements were performed on these thin films with a Veeco Dimension 3100 AFM connected to a Nanoscope IIIa controller equipped with an extender module, operating in the dark in ambient air. Ti/Pt-coated Si tips (NSC36/Ti-Pt, MikroMasch) with force constant of ~1 N/m, resonance frequency of ~100 kHz and apex radius of ~40 nm were used. Topographic images are taken in tapping mode (a.k.a. intermittent contact mode), potentials were measured by SKPM in lift mode with a typical lift height of 25 nm, using the amplitude modulation technique with an AC voltage modulation of 3 V superimposed on the DC tip potential. Care was taken that the scanning tip did not affect the polarization of the probed layers.

1.3 Preparation of N,N',N''-trioctadecylbenzene-1,3,5-tricarboxamide (**1**)**.** A 100 mL three-necked round-bottom flask was charged with a solution of octadecan-1-amine (3.34 g, 12.4 mmol), triethylamine (1.1 eq., 1.37 g, 13.6 mmol) in dry $CHCl_3$ (20 mL, stabilized with amylene) under inert atmosphere. A solution containing benzene-1,3,5-tricarboxylic acid chloride (0.3 equiv, 1.0 g, 3.77 mmol) in dry $CHCl_3$ (10 mL, stabilized with amylene) was slowly added dropwise to this solution while cooling with an ice bath. Subsequently, the ice bath was removed and the solution was stirred overnight under inert atmosphere. The reaction mixture was then transferred to a separating funnel and washed three times with 1M HCl (40 mL). The organic layer was collected and the solvent was removed *in vacuo*. The crude product was recrystallized from $CHCl_3$/ethanol (1:1) and obtained as a white solid (0.7 g, 73%). ^{1}H NMR ($CDCl_3$): δ = 8.33 (s, 3H, Ar-*H*), 6.41 (t, 3H, N-*H*), 3.47 (q, 6H, NHCH_2), 1.64–1.26 (m, 96H, CH_2), 0.90 (t, 9H, CH_3). ^{13}C NMR ($CDCl_3$): δ = 165.9, 135.5, 128.0, 40.6, 32.1, 29.9-29.5, 27.2, 22.8, 14.3. Elemental analysis: Calculated for $C_{63}H_{117}N_3O_3$: C, 78.44; H, 12.23; N, 4.36, found: C,

78.37; H, 12.23; N, 4.30. MALDI-TOF MS: Calculated: $[M+H]^+$ = 964.91 Da, observed: $[M+H]^+$ = 964.89 Da.

2 Calorimetric data.

Table S1. Phase Behavior of **1**.

Cycle	T, °C (ΔH, kJ/mol) [a]				
Heating	Cr	79 (74.1) [b]	Col_{hd}	210 (16.0)	I
Cooling	Cr	60 (90.8)	Col_{hd}	209 (14.6)	I

[a] Onset temperatures and transition enthalpies are reported based on the first cooling and second heating run in DSC (10 °C/min). The observed phases are identified by following abbreviations: Cr = crystalline, Col_{hd} = disordered hexagonal columnar LC, I = isotropic liquid.

[b] The main melting transition is preceded by a very broad and weak transition with a peak at 63 °C.

3 WAXS data and indexing.

Figure S1a shows the WAXS patterns recorded for **1** in the LC phase at 150 °C and after cooling from the LC phase at 40 °C. The characteristic reflections of the hexagonal lattice (see Figure S1b) and the interdisk distance between the BTAs along the column axis are clearly visible (also see Table S2).

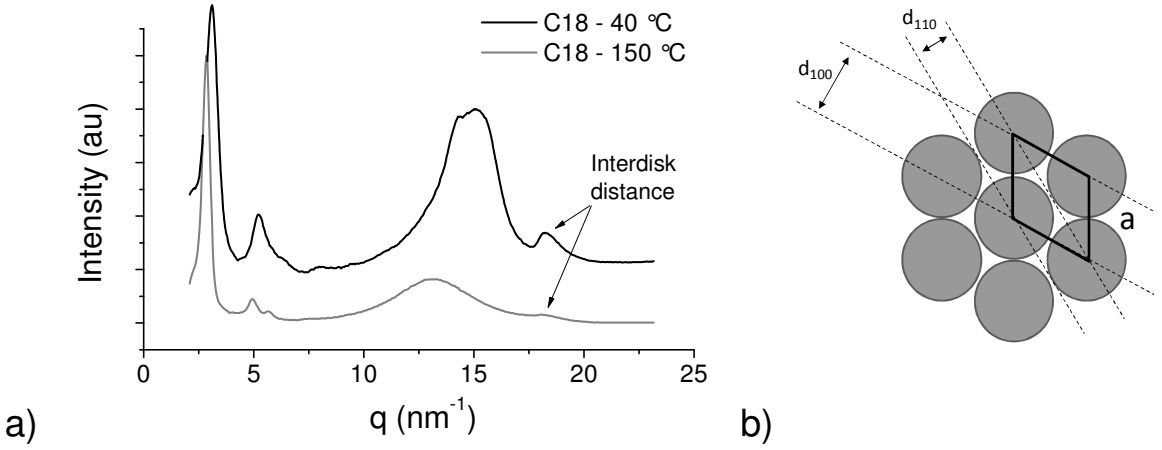

Figure S1. a) Integrated WAXS patterns for **1** at 40 °C and 150 °C; b) Schematic illustration of the hexagonal columnar lattice and its main spacings (unit cell in heavy black line).

Table S2. Indexation of the WAXS Data for **1**.

T (°C)	*hkl*	d_{obs} (nm)	d_{calc} (nm)	lattice type and parameters		
40	100	2.03	2.04	type:	Cr [a]	
	110	1.20	1.18	a =	2.36	nm
	200	1.01	1.02	c =	0.34	nm
	001	0.34		ρ [b] =	0.98	g/mL
150	100	2.21	2.21	type:	Col_{hd} (*p6mm*)	
	110	1.27	1.28	a =	2.55	nm
	200	1.11	1.10	c =	0.34	nm
	001	0.34		ρ =	0.84	g/mL

[a] The phase is crystalline, but the columnar nature and hexagonal arrangement of the columns as found in the LC phase remain intact.

[b] Calculated based on unit cell volume and molecular weight.

4 Full results switching experiments.

To determine the spontaneous polarization (P_s) and coercive field (E_c) that characterize the ferroelectric switching process in **1**, the observed polarization was plotted as a function of the applied electric field (Figure S2b). These *P*-*E* loops were constructed by integrating the cell response voltage as a function of time and using the known values of the measurement resistance, cell spacing and electrode area.[6] When the total area under the cell response curves is used for this procedure a total polarization is obtained that contains contributions from both the spontaneous polarization of the ferroelectric switching process as well as the conductive and capacitive effects (gray line in Figure S2b). Therefore, the values for the coercive field and residual polarization were estimated based on the area of the voltage peak due to polarization reversal by assuming a linear baseline under this peak (black line in Figure S2b, baseline indicated by dotted lines in Figure S2a). The parameters P_s and E_c were determined from the axis crossings of the *P*-*E* loops obtained in this manner.

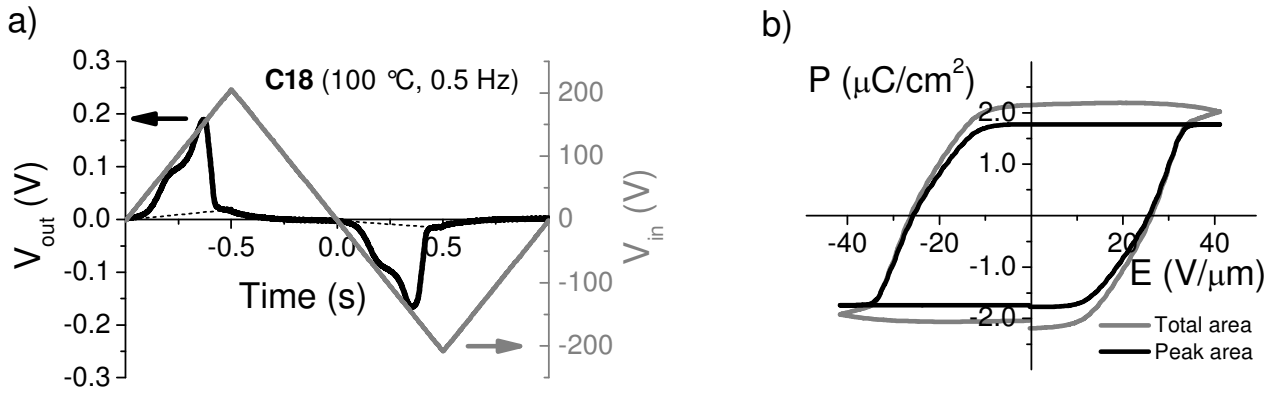

Figure S2. Results of the ferroelectric switching experiments under a triangular wave input voltage. a) The input voltage (dark gray, right axis) and the voltage over the measurement resistance resulting from the polarization current as function of time (black, left axis). Measurement conditions are noted on the top right and the baseline used for integration of the current peak is indicated by the dotted line; b) Polarization against field *(P-E* hysteresis loops) calculated from the data in a). The polarization evaluated based on the total area under measured voltage curves is plotted in dark gray and the polarization based solely on the area of the peak is plotted in black.

Table S3: Full Results for the Temperature Dependant Ferroelectric Switching Measurements.

T, °C	P_s, μC/cm² [a]	E_c, V/μm [a]	F_{max}, Hz [b]
70	1.6 ± 0.2	25.8 ± 0.3	0.1
100	1.7 ± 0.1	25.2 ± 0.9	0.5
120	1.6 ± 0.1	23.1 ± 1.5	1.0
150	1.4 ± 0.1	21.0 ± 1.1	5.0

[a] Values are averaged over at least three measurements from at least two unique cells. The reported error margin is the standard deviation of the measured values.

[b] Maximum driving frequency that allowed the polarization to saturate at the given temperature. All measurements were conducted at or slightly below this frequency.

5. Typical cell response in lifetime measurements.

The total polarization (P_r) was determined by integrating the current peak from $t = 0$ (application of the probe pulse) up to $t = t_e$ (polarization of the sample completely built-up) after correcting for the RC-contribution (5-10 μs) and the background caused by ohmic conduction. The time t_e was determined as the crossing point of two lines constructed by linear extrapolation of the right edge of the peak and the background signal due to conduction on a double-logarithmic scale (see Figure S3a and b)

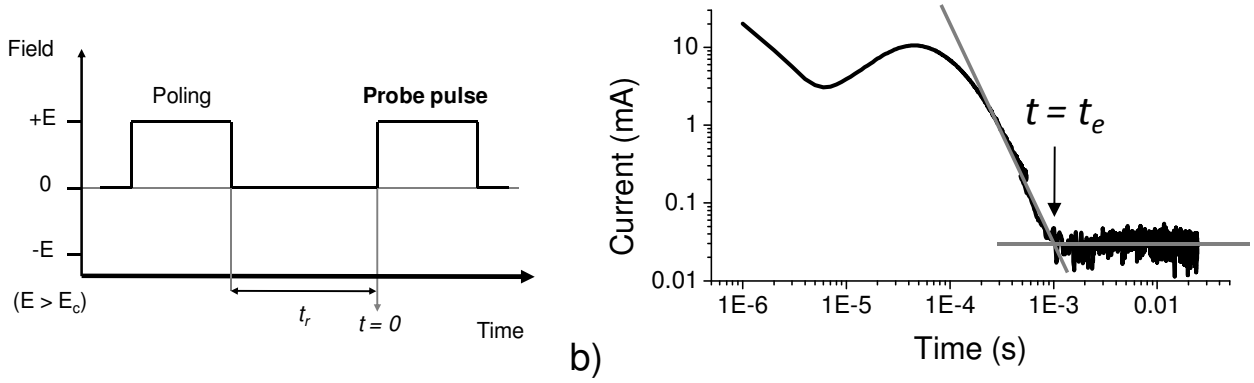

Figure S3. a) Schematic representation of the pulse sequence used for measurement. b) Typical cell response to the application of a second, probe pulse after a time interval t_r. The determination of $t = t_e$ (polarization of the sample completely built-up) is shown by gray lines.

6. Additional SKPM and AFM data.

Figure S4 shows representative examples of large scale (10x10 μm) AFM images obtained for unaligned and aligned samples areas of thin films of **1**. The surface potential histograms in Figure 2d in the main text were constructed from the SKPM images in Figure S5, which present typical results for the surface potential measurements on thin films of **1**.

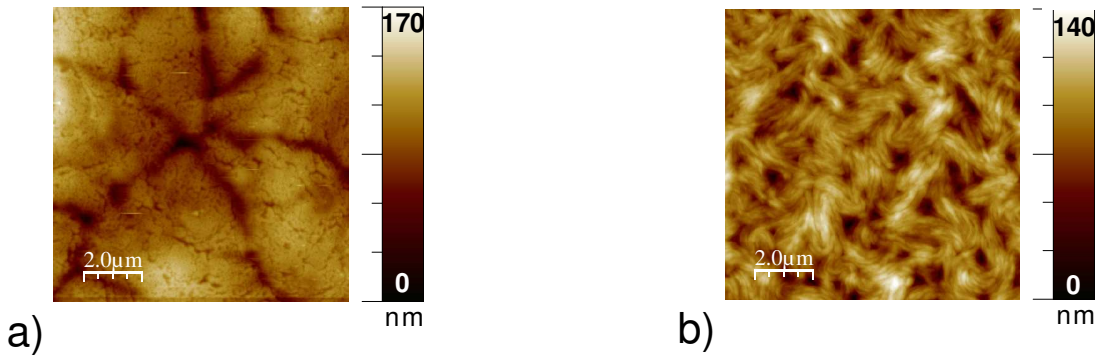

Figure S4. AFM images (10x10 µm) of a) aligned and b) unaligned thin films of **1**.

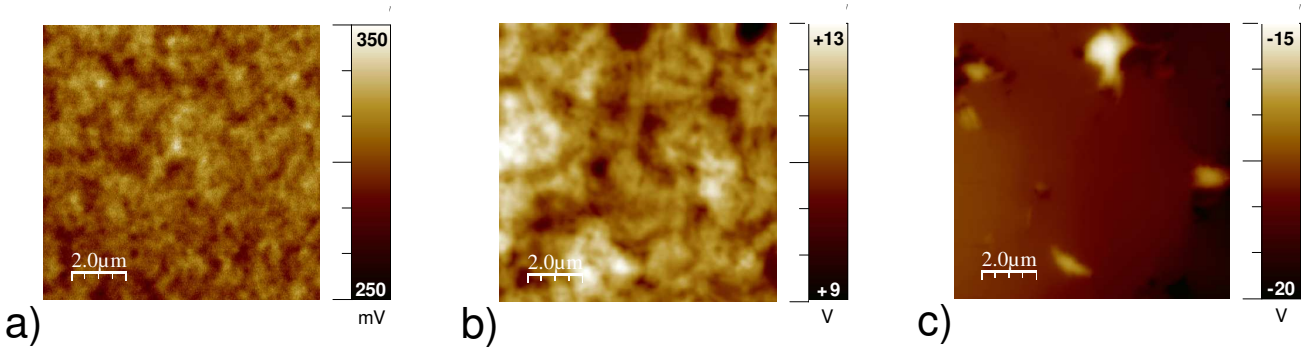

Figure S5. Typical SKPM images for the a) unpoled, b) negatively poled, and c) positively poled thin films of **1**.

7. Reference and notes.

(1) Hammersley, A. P.; Svensson, S. O.; Hanfland, M.; Fitch, A. N.; Hausermann, D. *High Pressure Res.* **1996**, *14*, 235-248.

(2) Francescangeli, O.; Stanic, V.; Torgova, S. I.; Strigazzi, A.; Scaramuzza, N.; Ferrero, C.; Dolbnya, I. P.; Weiss, T. M.; Berardi, R.; Muccioli, L.; Orlandi, S.; Zannoni, C. *Adv. Funct. Mater.* **2009**, *19*, 2592-2600.

(3) Angell, C. A. *Science* **1995**, *267*, 1924-1935.

(4) Glusen, B.; Kettner, A.; Kopitzke, J.; Wendorff, J. H. *J. Non-Cryst. Solids* **1998**, *241*, 113-120.

(5) Russell, E. V.; Israeloff, N. E. *Nature* **2000**, *408*, 695-698.

(6) Strictly speaking, the combined current flow resulting from the conductance of the samples and the dielectric displacement (*D*) are measured, the latter of which consists of a vacuum and a material contribution. The polarization (*P*) refers to the part of the dielectric displacement that originates from the response of the material to the electric field only. Since the value of the spontaneous polarization of the BTAs is estimated by subtracting a baseline that takes both conductive and capacitive effects into account, the term 'polarization' is used throughout this paper to avoid confusion.